Applied Surface Science 374 (2016) 96–103

Contents lists available at ScienceDirect

Applied Surface Science

journal homepage: www.elsevier.com/locate/apsusc

Optical properties of polydimethylsiloxane (PDMS) during nanosecond laser processing

N.E. Stankova[a,*], P.A. Atanasov[a], Ru.G. Nikov[a], R.G. Nikov[a], N.N. Nedyalkov[a], T.R. Stoyanchov[a], N. Fukata[b], K.N. Kolev[c], E.I. Valova[c], J.S. Georgieva[c], St.A. Armyanov[c]

[a] Institute of Electronics, Bulgarian Academy of Sciences, 72 Tsaridradsko shose Boul., Sofia 1784, Bulgaria
[b] International Center for Materials for NanoArchitectonics (MANA), National Institute for Materials Science (NIMS), 1-1 Namiki, Tsukuba 305-0044, Japan
[c] Rostislaw Kaischew Institute of Physical Chemistry, Bulgarian Academy of Sciences, Acad. G. Bonchev Str., Block 11, Sofia 1113, Bulgaria

ARTICLE INFO

Article history:
Received 24 June 2015
Received in revised form 7 September 2015
Accepted 4 October 2015
Available online 9 October 2015

Keywords:
PDMS elastomer
UV
VIS and NIR nanosecond laser processing
Incubation
Optical transmittance
μ-Raman analysis

ABSTRACT

This article presents experimental investigations of effects of the process parameters on the medical grade polydimethylsiloxane (PDMS) elastomer processed by laser source with irradiation at UV (266 and 355 nm), VIS (532 nm) and NIR (1064 nm).

Systematic experiments are done to characterize how the laser beam parameters (wavelength, fluence, and number of pulses) affect the optical properties and the chemical composition in the laser treated areas. Remarkable changes of the optical properties and the chemical composition are observed. Despite the low optical absorption of the native PDMS for UV, VIS and NIR wavelengths, successful laser treatment is accomplished due to the incubation process occurring below the polymer surface.

With increasing of the fluence and the number of the pulses chemical transformations are revealed in the entire laser treated area and hence decreasing of the optical transmittance is observed. The incubation gets saturation after a certain number of pulses and the laser ablation of the material begins efficiently. At the UV and VIS wavelengths the number of the initial pulses, at which the optical transmittance begins to reduce, decreases from 16 up to 8 with increasing of the laser fluence up to 1.0, 2.5 and 10 J cm^{-2} for 266, 355 and 532 nm, respectively. In the case of 1064 nm the optical transmittance begins to reduce at 11th pulse incident at a fluence of 13 J cm^{-2} and the number of the pulses decreases to 8 when the fluence reaches value of 16 J cm^{-2}. The threshold laser fluence needed to induce incubation process after certain number of pulses of 8 is different for every wavelength irradiation as the values increase from 1.0 for 266 nm up to 16 J cm^{-2} for 1064 nm. The incubation and the ablation processes occur in the PDMS elastomer material during its pulsed laser treatment are a complex function of the wavelength, fluence, number of pulses and the material properties as well.

1. Introduction

Silicone-based elastomer polydimethylsiloxane (PDMS) is one of the most popular technical polymeric materials due to its advantageous properties: simple and inexpensive fabrication process, mechanical flexibility and stability, high dielectric constant and breakdown field, optical transparency in the UV, VIS and NIR spectral regions, high biocompatibility and biostability. PDMS is widely used in the fabrication of various micro-electro-mechanical systems (MEMS) and nano-electro-mechanical systems (NEMS) devices such as lab-on-a-chip, waveguides and memory-based devices [1–4], dielectric elastomer actuators [5], as well as in numerous pharmaceutical and medical applications [6–8]. Owing to its remarkable properties, the PDMS-elastomer is also used in biomedicine as encapsulation and/or as substrate insulator carrier for long term neural implants [9,10]. Highly flexible polymeric microelectrode arrays (MEAs) based on PDMS-elastomer scaffold composed by micro-channeled tracks as electrodes are applied as neural interfacing technologies for monitor and/or stimulation of neural activity [11–14]. Elastomeric MEAs can be rolled and flexed, thus offering an improved structural interface with neural tissues. Hence, the modification or structure formation of the PDMS elastomer surface opens an interesting research field for different applications.

Laser ablation of polymers is a well established process in industrial applications as an alternative to the traditional lithographic methods. Direct laser writing (DLW) based on multiphoton polymerization has been proposed for the production of 3D

* Corresponding author.
E-mail address: nestankova@yahoo.com (N.E. Stankova).

http://dx.doi.org/10.1016/j.apsusc.2015.10.016
0169-4332/

micro/nanostructures in 1997 [15]. UV, VIS and NIR ns- and fs-laser irradiation of PDMS-elastomer under ambient conditions is an easy and powerful method of micromachining allowing activation and functionalization of the surface without altering its bulk properties [3,15–28]. Laser micromachining is based on the laser direct ablation, which appears as a very suitable, low cost and versatile controlled processed parameters technique for the fabrication of tracks and complex 2D/3D structures with dimensions of several tens of microns or less in wide range of materials. Consequently, this approach allows the numbers of electrodes and pads to be increased by miniaturization of the tracks on the PDMS substrate and thus, to increase the nerve selectivity. After laser processing, selective metallization of the as-processed surface is obtained by immersion of the sample into autocatalytic bath containing metal ions (Ni or Pt) [27,28].

PDMS belongs to the specific class of polymers that are based on Si atoms. They are constituted of Si—O chains to which CH_3-radicals are fixed via Si—C bonding. In spite of the high transmittance in UV–VIS–NIR range of the spectra, it is possible to modify the surface of the PDMS elastomer by lasers irradiating in this range. This process is possible because incubation occurs below the surface by local chemical transformations. Apparently, the incubation effects are significant for the weakly absorbing materials such as the PDMS polymer. Under the laser exposure the polymer undergoes substantial degradation that alters its optical properties, making the material much more absorptive. It results in increase of the linear absorption coefficient and decrease of the laser fluence, which should be delivered in order the ablation to begin. Different mechanisms (photothermal and photochemical) are proposed in terms of the dependence of the dynamics of the etching process on the laser fluence, wavelength, pulse length, number of pulses (incubation), and the intrinsic properties of the polymer materials [29–33], and details of quantitative understanding are still controversial. Some authors declared that both photothermal and photochemical mechanisms contribute to the ablation at low laser fluences. Moreover, defects creation into the material, i.e. incubation, is considered as responsible for laser ablation of polymers.

In this work we seek to characterize and compare the optical properties of the PDMS elastomer processed by NIR, VIS, and UV pulsed ns-laser irradiation. The study is focused on understanding of the effects of three main process parameters – wavelength, laser fluence and pulse overlapping – on the optical absorption (incubation process), ablation depth, and chemical composition changes in order to activate the surface for further successful metalization of the tracks. Our work can enrich the discussion about laser induced changes in thin PDMS sheets which can be exploited in the context of the direct laser writing of microchannels for applications as microelectrode arrays (MEAs) in neural interfacing technologies for monitor and/or stimulation of neural activity.

2. Experimental

170 μm thick medical grade PDMS elastomer sheets (MED 4860) are irradiated with the fundamental frequency (FF, 1064 nm), second (SH, 532 nm), third (TH, 355 nm) and fourth (FH, 266 nm) harmonics of a Q-switched Nd:YAG (pulse duration $\tau = 15$ ns and repetition rate of 1–10 Hz) laser in air environment. The laser beam is focused normally on the PDMS surface by lens with focal length of 22 cm. The laser spot diameter is between 1.0 and 1.3 mm. The laser fluence increases from 0.5 to 16 J cm^{-2} depending on the laser wavelength applied. The data of the processing laser parameters are shown in Table 1. The samples are mounted on a stepper-motor *x*-*y* table with minimum step of 12.7 μm. The experimental setup configuration allows structuring of a single spot or a single line on the sample surface by pulsed laser ablation when the translational table is at standstill or the sample is translated along *x*- or *y*-axis, respectively. Single spot ablation is performed by applying of different number of pulses from 1 to 110 pulses with repetition rate of 1 Hz.

Table 1
Summary of the laser processing parameters. Comparison of the linear absorption coefficient and the average ablation depth. The absorption coefficient and the penetration depth are calculated according to the Beer–Lambert law, as the scattering is ignored, i.e. the values represent the linear absorption coefficient.

Wavelength	266 nm	355 nm	532 nm	1064 nm
Laser fluence (J cm^{-2})	0.5–1.0	2.0–4.0	7.0–10.0	13.0–16.0
α (cm^{-1})	14.9	7.38	3.58	2.86
Penetration depth (μm)	669	1354	2794	3502
Ablation depth (μm)	40	72	134	150

Continuous linear tracks are obtained by overlapping of each adjacent spot of the laser beam on the surface so as every unit of area is treated by 22 or 33 consecutive pulses. The moving speed of the *x*-*y* table is determined according to the number of pulses needed to perform at a unit of area and the laser repetition rate.

Before the laser treatment the PDMS samples are cleaned by the following steps: cleaning in a detergent solution using ultrasound bath; rinsing with deionized water; again cleaning with ethanol in ultrasound bath; and air stream drying finally.

The experimental techniques applied for characterization of the PDMS samples are: optical spectroscopy (Ocean Optics HR 4000 spectrophotometer) for measurements of the optical transmission in the near ultraviolet (UV), visible (VIS) and near infrared (NIR) range of the spectra; optical microscopy (Zeiss Opton) for observation of any visible permanent modifications of the surface and measurement of the ablation depth; VK-9700K Color 3D laser Microscope (KEYENCE) for viewing and analyzing of the laser treated areas; μ-Raman spectroscopy (RMS-310 μ-Raman spectrometer (Photon Design)) equipped with laser source operating at $\lambda = 532$ nm for determination of the chemical composition and scanning electron microscope (SEM) SEM/FIB (Lyra/Tescan dual beam system) for the assessment of the laser tracks.

3. Results and discussion

We chose to work with thin medical grade PDMS sheets in accordance to the small size requirements of the potential application as implantable medical devices (neural or muscular surface interfacing). The changes of the optical properties of the PDMS samples after laser irradiation with different wavelengths (266, 355, 532, and 1064 nm) and different number of pulses in single spot ablation mode at various laser fluences are investigated by measuring of the optical transmittance (Fig. 1). It is known that the native medical grade silicones as PDMS elastomer are optically transparent from the near UV up to NIR region of the spectra. Laser treatment of such materials with wavelengths in this spectral region is possible because of the effect of incubation process attributed to increase optical absorption due to accumulation of damages or defects below the surface. It is considered that the incubation in the polymers is a result from the chemical transformations (intermolecular bonds breaking) occur in the local area laser treated without changing the bulk material properties. These modifications depend simultaneously on the wavelength and the laser fluence applied, and appear after a certain number of pulses. It means at given wavelength and laser fluence, the absorption increases during the laser irradiation with the initial incident pulses, i.e. certain number of pulses is required to accumulate local chemical transformations and to reach the ablation conditions.

In our experiments any visible permanent modification of the laser treated area of the PDMS surface observed by optical microscope at 625× magnification is defined as ablation. At a given

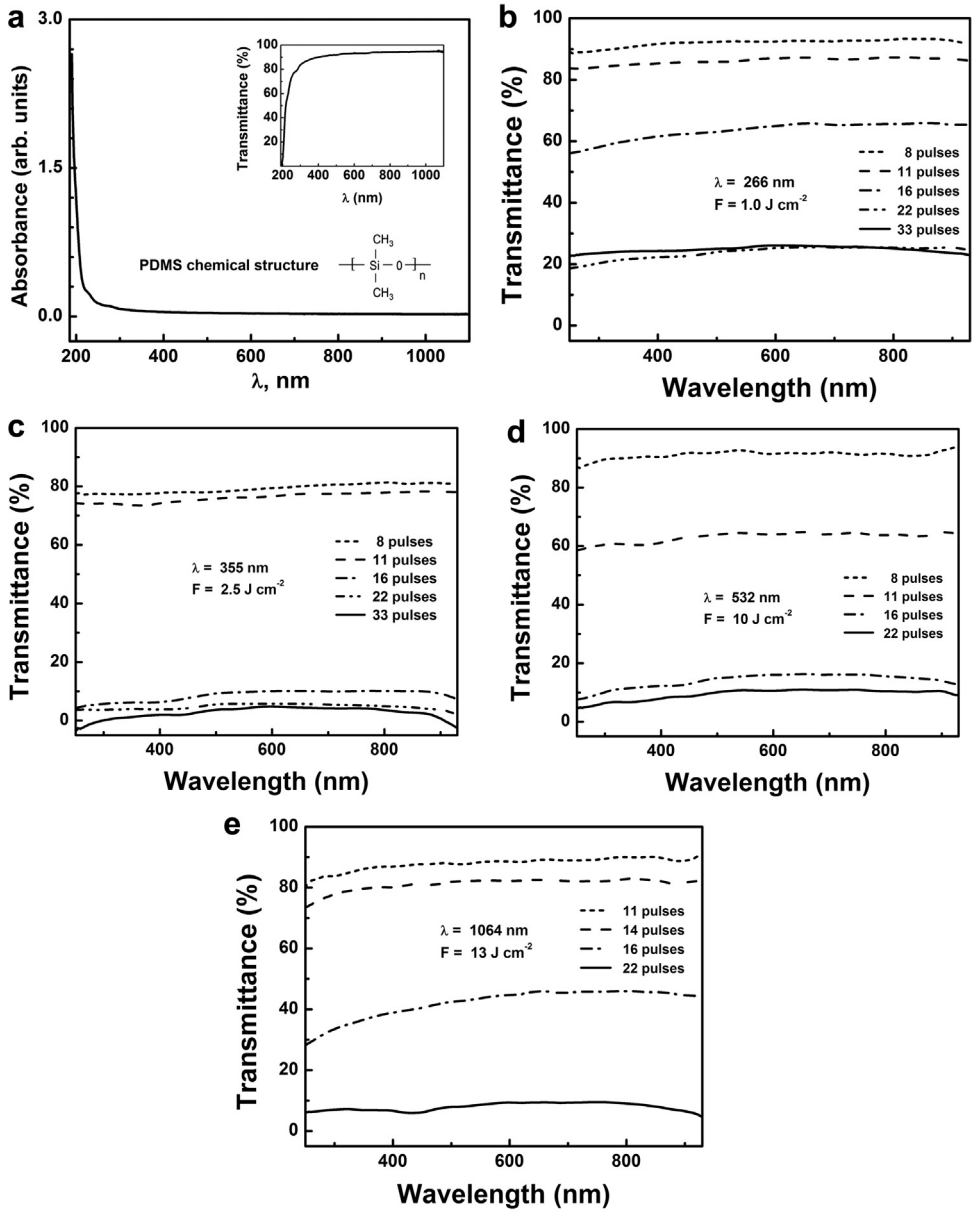

Fig. 1. Optical properties spectra: (a) UV–VIS–NIR absorbance and transmittance of the native medical grade PDMS samples (thickness of 170 μm). Optical transmittance of the PDMS areas laser treated by irradiation at (b) 266 nm, (c) 355 nm, (d) 532 nm, (e) 1064 nm, and different number of pulses and fluences. Incubation effect begins at the 8th pulse for UV and VIS light and at 11th pulse for NIR light. Incubation saturation occurs at the 22nd pulse.

wavelength the number of the initial pulses, at which the optical transmittance begins to reduce (i.e. optical absorption increases; Fig. 1(b)–(e)), decrease with increasing of the laser fluence. The investigation of the optical properties shows that at 266 and 355 nm the optical transmittance begins to decrease rapidly after the 8th pulse emitted at the fluences of 1.0 and 2.5 J cm^{-2}, respectively. Whereas at the lowest values of the fluence it happens after the 16th shot at 266 nm and after the 11th pulse at 355 nm. In the case of the visible wavelength (532 nm) the optical transmittance decreases after the 8th pulse emitted at the highest fluence of 10 J cm^{-2} applied. At the lower flunces between 9 and 7 J cm^{-2} this behavior is observed between 11th and 16th pulses incident, respectively. At 1064 nm the number of the pulses incident, which cause the optical transmittance reduce, are 11 at the lowest laser fluence of 13 J cm^{-2} applied, and decreases up to 8 with increasing of the fluence to 16 J cm^{-2}. It could be explained by the higher energy delivered to the sample spot from every consecutive pulse, which accumulates chemical modifications enough below the surface. Comparison of the optical microscope images of the laser treated spots with different laser parameters are presented in Fig. 2. It is seen that after irradiation with pulses up to 16 the chemical transformations (the visible damages) and the microstructuring below the surface are still distributed nonuniform. With increasing of the number of the pulses the defects occur almost in the entire area laser treated and the ablation and ablation products are clearly visible. Strong decrease of the optical transmittance could be explained by the certain amount of chemical modifications occurring in the laser treated area, which, respectively, leads to high increase of the optical absorption. It means the incubation in this area saturates and the laser ablation of the material begins efficiently.

We observed that the lowest number of the incubation pulses (at which the changes mentioned above are observed) is eight (8) for all four wavelengths applied but different laser fluencies are needed to deliver (Fig. 1(b)–(e)). The fluence at which the incubation begins at the 8th pulse emitted and the optical transmittance starts decreasing in the case of processing with the wavelength of

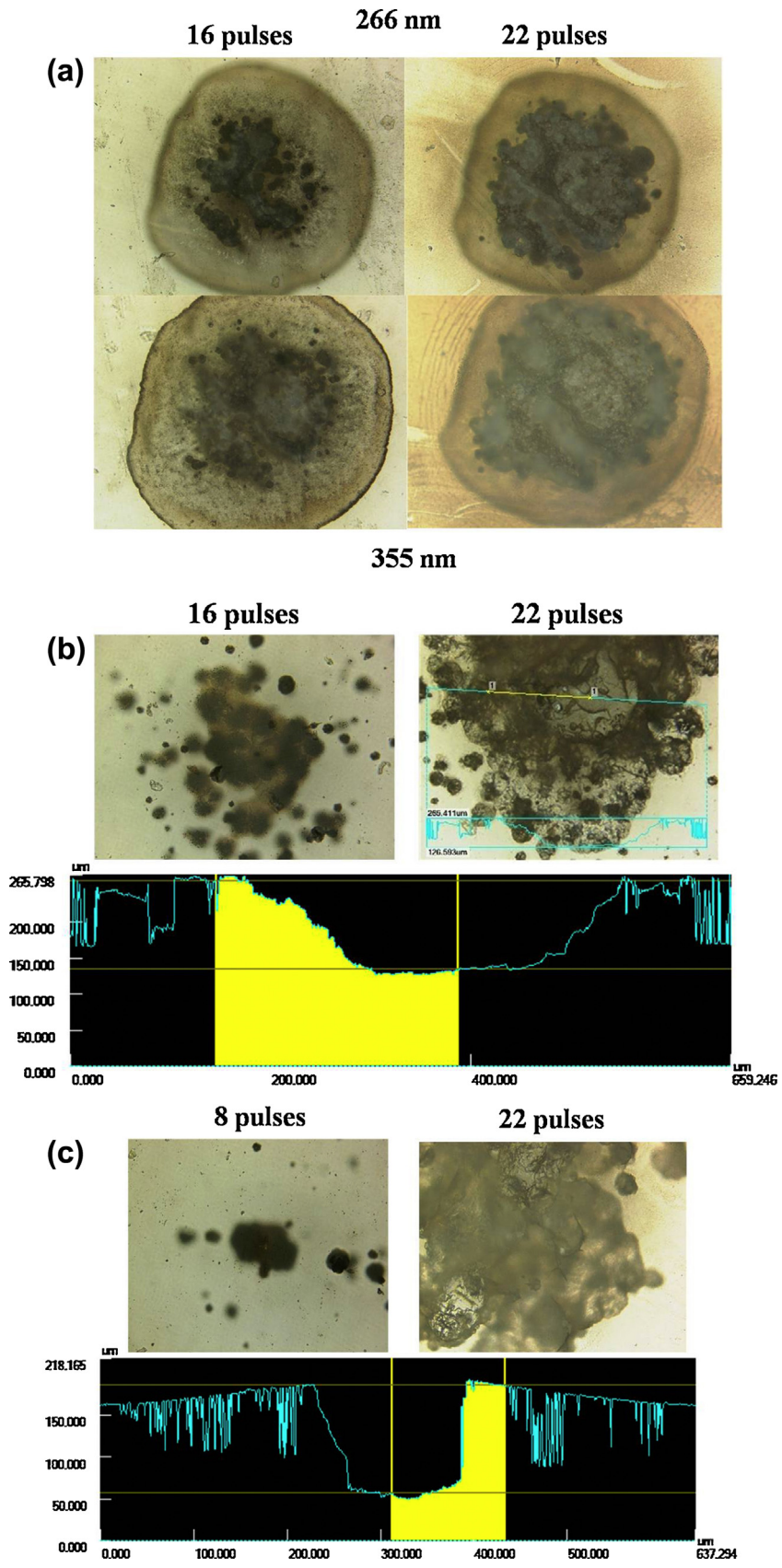

Fig. 2. Laser microscope images of irradiated PDMS samples with: (a) UV (266 and 355 nm); (b) VIS (532 nm); and (c) NIR light (1064 nm) with fluences of 1.0, 2.5, 10 and 13 J cm^{-2}, respectively. The microscope is focused onto the surface. Chemical transformations located below the surface appear less sharp. Areas of ablation and the ablation products are apparent.

266 nm is the lowest one –1.0 J cm^{-2}. Whereas, the energy density, which causes visible damages at the same number of pulses emitted at the fundamental wavelength, is much higher about 16 J cm^{-2}. Under irradiation with wavelengths of 355 and 532 nm the incubation begins at the 8th pulse at fluences of 2.5 and 10.0 J cm^{-2}, respectively. The transmittance decreases gradually with further increasing of the number of the pulses and at 22 pulses and higher the material becomes almost opaque in the entire area laser treated with UV and VIS wavelengths (266, 355, and 532 nm) at fluences of 1.0, 2.5 and 10 J cm^{-2}, respectively (Fig. 1(b)–(d)). Whereas, at 1064 nm the laser treated area becomes opaque at lower number of pulses – at the 14th pulse emitted (at fluence of 16 J cm^{-2}). It must be noted that at 532 nm irradiation with pulses more than 22 the sample is drilled, while at 1064 nm this effect occurs earlier – after the 14th pulse at the fluences mentioned above. Drilling of the material irradiated with both UV laser lights with parameters, at which incubation reveals at the eighth pulse, is observed after pulses more than 110. It should be noted that in the case of NIR irradiation, the PDMS sample becomes opaque at the 22nd pulse when the laser fluence decreases up to 13 J cm^{-2}. However, at this fluence the incubation begins after higher number of the pulse (11) and after the 22nd pulse emitted the material is drilled.

Much higher values of the laser fluence needed to induce incubation process in the PDMS material by VIS (532 nm) and NIR (1064 nm) light irradiation could be explained by the lower photon energies of 2.3 and 1.2 eV, respectively, in comparison with the UV photon energies of 4.7 and 3.5 eV for wavelengths of 266 and 355 nm, respectively. Despite the low optical absorption (linear absorption coefficient, Table 1) of the PDMS elastomer to the photons with energy in the range of 5.0–1.2 eV (248–1064 nm wavelength range, respectively), UV photons are probably absorbed selectively and exclusively onto Si—C electron bonds with binding energy of 3.3 eV. It is expected organic radicals to be ejected as a result from the laser irradiation of the surface, while the backbones Si—O and C—H bonds, which have higher binding energy of 4.7 eV and 4.3 eV, respectively, could be broken with higher fluence. Obviously, much higher energy should be delivered into the laser treated area in order the corresponding chemical bonds to be broken and the material to be ablated by using VIS and NIR irradiation light. This assumption is confirmed by the μ-Raman spectroscopy measurements performed.

Furthermore, the drilling observed at the significant lower number of pulses performed for the wavelengths of 532 and 1064 nm is probably due to the occurrence of incubation effects below the surface in a depth deeper than the depth at which the UV light penetrates. This is a consequence of the lower absorption coefficient of the native PDMS in the VIS–NIR region in comparison with UV region of the spectra, which results in higher penetration depth of the longer wavelengths in the sample (Fig. 1(a)). The laser ablation depth of the spots processed by the four laser wavelengths (266, 355, 532, and 1064 nm), 22 pulses, and fluences of 1.0, 2.5, 10, and 13 J cm^{-2}, respectively, is the highest (~150 μm) at 1064 nm, and gradually decreases with the wavelength decrease. The ablation depth reaches the lowest value (~40 μm) at 266 nm, the summarized data are provided in Table 1. In addition to the material structural properties influence, different mechanisms of ablation (photothermal and photochemical) also can contribute significantly to the different depth and the width of the etched holes, when the PDMS sample is processed by different laser parameters (wavelength and fluence). Therefore the ablation depth (as a result from the incubation process in the PDMS elastomer samples) is a complex function simultaneously of the wavelength, fluence, number of pulses and the material properties.

The results obtained show that direct laser writing on PDMS elastomers for production of microchannels for applications as microelectrode arrays (MEAs) in neural interfacing technologies could be performed successfully by laser sources irradiating in UV, VIS or NIR range of the spectra with exposure parameters appropriately selected.

Linear tracks in PDMS material with depth between 40 and 150 μm and width higher than 1000 μm (because the laser beam spot is higher than 1000 μm) are performed by laser irradiation at all four wavelengths, 22 consecutive number of overlapping pulses, and laser fluences of 1.0, 2.5, 10, and 13 J cm^{-2}, respectively. Optical microscope and SEM measurements showed uniform laser processed tracks. Microchannels with different size (depth and width) in micron and submicron scale can be produced by varying of the laser beam parameters. It could be considered that UV laser processing of medical grade PDMS elastomer is more appropriate than VIS and NIR lights in accordance to the fine size and high density requirements of the electrode channels in terms of the ability to provide safe stimulation at high resolution of implantable interfacing devices such as neuroprostheses [14].

Typical Raman spectrum of the native PDMS elastomer material shows following peaks characterizing the various chemical bonds: 488 cm^{-1} (Si—O—Si symmetric stretching); 685 cm^{-1} (Si—CH_3 symmetric rocking); 709 cm^{-1} (Si—C symmetric stretching); 787 cm^{-1} (CH_3 asymmetric rocking + Si—C asymmetric stretching); 859 cm^{-1} (CH_3 symmetric rocking); 1262 cm^{-1} (CH_3 symmetric bending); 1411 cm^{-1} (CH_3 asymmetric bending); 2909 cm^{-1} (CH_3 symmetric stretching); and 2970 cm^{-1} (CH_3 asymmetric stretching) [34]. The chemical composition of the laser treated spots of PDMS elastomer is investigated by μ-Raman spectroscopy. The spectra acquired after the measurements in different points in the laser treated area (where the chemical transformations occured) differ significantly from the spectrum of the native PDMS sample (Fig. 3). Regardless the laser wavelength applied strong and sharp peak between 515 and 519 cm^{-1} appears in all spectra, which can be attributed to mono and/or polycrystalline or only to monocrystalline silicon (c—Si) [35]. Its intensity increases with increasing of the laser fluence and becomes more dominant with further rise of the number of pulses, while the intensity of the Si—O—Si peak at 488 cm^{-1} decreases. It could be due to the reduction of the Si—O—Si bonds by breaking of the Si—O bond and as a result Si crystallites are formed. Also the intensity of the peaks at 685, 709, 787 and 859 cm^{-1} decreases, which reveals that the Si—CH_3, Si—C and CH_3 bonds are broken and probably it contributes to the c—Si formation. The weak broad peak between 936 and 960 cm^{-1} can be ascribed to the microcrystalline Si—C bond [36]. It is better expressed in the VIS and NIR laser irradiated areas.

Two wide but pronounced peaks in the range of 1330–1336 and 1590–1615 cm^{-1}, respectively, are observed in the Raman spectra of some points of the areas treated with both UV lights with number of pulses higher than 33. It is seen that the high signal on the peaks tails hinders the other Raman features (Fig. 3(a)). In the cases of the VIS and NIR irradiation these two peaks are much less expressed, which could be a result from the irradiation with number of pulses lower than 33. The Raman spectra of carbons according to the literature contain two peaks called D and G modes, which lie at around 1360 and 1560 cm^{-1} at visible excitation. They are attributed to the disordered carbon with sp^2 bonds [37]. It is known that amorphous carbon contains a mixture of sp^3, sp^2 and sp^1 sites. These two peaks dominate, because sp^2 sites have cross section much higher (~55) than this one of the sp^3 sites at the visible excitation of 514 nm. It is worth noting that only for high quantity of the sp^3 sites (which are related to the diamond phase) the D peak can be seen at 1332 cm^{-1} (Raman peak of phase mixed by the hexagonal and the cubic diamond could be extended in the range between 1300 and 1350 cm^{-1} [38]), which is usually broadened and lowered because of the phonon confinement at visible excitation. Also, the investigations show that carbon materials, which contain simultaneously sp^2 and sp^3 phases, reveal shift of the G band over the 1600 cm^{-1}

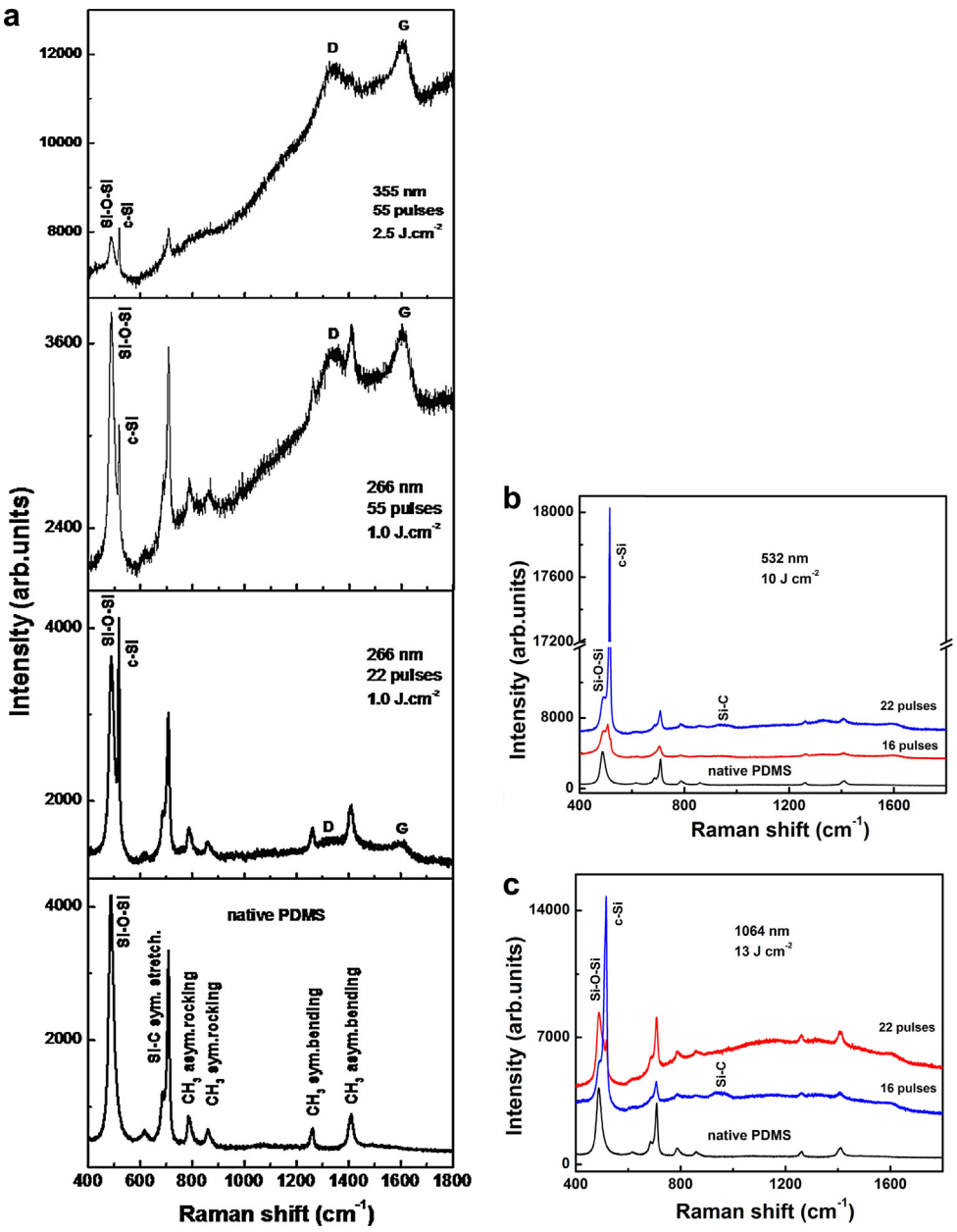

Fig. 3. μ-Raman spectra of native and ns-laser processed PDMS-elastomer with laser (a) UV, (b) VIS and (c) NIR irradiation. Laser beam parameters are presented in the figures.

[37,39]. Hence, it could be concluded that the laser treated areas of PDMS elastomer, especially with UV light (266 and 355 nm) contain significant fraction of sp^3 carbon bonds.

The formation of inorganic products (silicon and carbon) after the laser processing of the PDMS material certainly proves the actual chemical activation of the surface. Obviously, the treatment of the PDMS material with all four laser wavelengths causes chemical transformation, i.e. silicone decomposition, irrespective of the corresponding photon energies applied. This behavior is due to rather the significant contribution of the higher energy delivered by increasing the laser fluence and/or the number of the pulses than only to the wavelength.

The chemical activation of the surface is expected to influence significantly the nucleation and the growth rate of the corresponding metal layer (usually it is Pt) during the following process of metallization, which is related to the adhesion and the thickness of the electrode arrays and hence to the DC resistance of the laser tracks.

4. Conclusions

The results of our investigation of the surface modifications after processing of PDMS-elastomer by ns-laser irradiation with four wavelengths (266, 355, 532 and 1064 nm) with different laser fluence and number of pulses can be summarized as follows. Investigation of the optical properties revealed that incubation occurs by local chemical transformations after a certain number of pulses emitted below the surface enough of the laser treated area without changing the bulk material properties. As a consequence decreasing of the optical transmittance in the area laser treated is observed. With increasing the number of the pulses the chemical modifications (the intermolecular bonds breaking) occurs in the entire laser treated area, the optical absorption highly increases, which leads to saturation of the incubation, and hence the laser ablation begins efficiently. At a given wavelength the number of the initial pulses, at which the optical transmittance begins to reduce,

decrease from 16 to 8 with increasing of the laser fluence up to 1.0, 2.5 and 10 J cm^{-2} for 266, 355 and 532 nm, respectively. The number of pulses decreases from 11 to 8 when the laser fluence increases from 13 to 16 J cm^{-2} at wavelength of 1064 nm. The threshold laser fluence needed to induce incubation process after certain number of pulses (eight) is different for every wavelength irradiation as the values increase from 1.0 for 266 nm up to 16 J cm^{-2} for 1064 nm. The ablation depth is the highest (~150 μm) for 1064 nm and decreases with decreasing of the wavelength (~40 μm for 266 nm). This is related to the lower linear absorption coefficient of the native material and the higher penetration depth of the laser light at the NIR wavelength. The incubation and the laser ablation depth depend simultaneously on the wavelength, the laser fluence, the number of the pulses applied and the material properties. Direct laser writing on PDMS elastomers for production of microchannels for applications as microelectrode arrays (MEAs) in neural interfacing technologies could be performed successfully by laser sources irradiating in UV, VIS and NIR range of the spectra with exposure parameters appropriately selected.

μ-Raman characterization revealed that chemical activation by decomposition of the silicone and formation of inorganic products (silicon and carbon) is occurred after treatment of the surface with UV, VIS and NIR laser irradiation, irrespective of the corresponding photon energies applied. Strong decrease of the intensities of the Si—O—Si stretching mode at 488 cm^{-1}, Si—CH_3 symmetric rocking at 685 cm^{-1}, Si—C symmetric stretching at 709 cm^{-1}, CH_3 asymmetric rocking + Si—C asymmetric stretching at 787 cm^{-1}, and CH_3 symmetric rocking at 859 cm^{-1} modes is observed, since the corresponding chemical bonds are broken by the laser irradiation. As a result important features are defined, such as: (i) Si crystallites are formed; (ii) amorphous carbon containing sp^2 and sp^3 sites is formed during the laser activation of the surface. sp^3 Bonds could be related to the presence of nanocrystallites of diamond phase in the laser treated area; and (iii) the local chemical decomposition is a complex function rather of the laser fluence, the number of the pulses (incubation) and the material properties than only of the wavelength.

Our results show promising prospects with respect to apply such methods of laser-based micro- or nano-fabrication of tracks by using direct laser writing with irradiation in the UV, VIS and NIR range of the spectra on PDMS-elastomer surface without using a mask. The further successful metallization of the tracks will give high definition devices used as MEMS, NEMS and MEAs, having applications for implantable neural interfacing technologies for monitor and/or stimulation of neural activity.

Acknowledgements

The authors express their acknowledgments to financial support of the BNSF under the project T02/24 entitled “New advanced method for processing nanocomposite materials for creation of microsystems for medical and high-tech applications”. Bilateral joint research project “Laser-based micro and nanoprocessing of materials relevant to functional applications” between Bulgarian Academy of Sciences (BAS) and Romanian Academy of Sciences (RAS) 2014–2016 is also acknowledged.

References

[1] A. Asgar, S. Bhagat, P. Jothimuthu, I. Papautsky, Photodefinable polydimethylsiloxane (PDMS) for rapid lab-on-a-chip prototyping, Lab Chip 7 (2007) 1192–1197.
[2] L. Narayana, D. Kallepalli, V.R. Soma, N.R. Desai, Femtosecond-laser direct writing in polymers and potential applications in microfluidics and memory devices, Opt. Eng. 51 (7) (2012) 073402.
[3] K.L.N. Deepak, S. Venugopal Rao, D. Narayana Rao, Femtosecond laser-fabricated microstructures in bulk poly(methylmethacrylate) and poly(dimethylsiloxane) at 800 nm towards lab-on-a-chip applications, Pramana – J. Phys. 75 (6) (2010) 1221–1232.
[4] K. Liu, Z. Nickolov, J. Oh, H. Moses Noh, KrF excimer laser micromachining of MEMS materials: characterization and applications, J. Micromech. Microeng. 22 (1) (2012) 015012.
[5] S. Rosset, H.R. Shea, Flexible and stretchable electrodes for dielectric elastomer actuators, Appl. Phys. A: Mater. Sci. Process. 110 (2013) 281–307.
[6] A. Colas, J. Curtis, in: B.D. Ratner, A.S. Hoffman, F.J. Schoen, J.E. Lemans (Eds.), Biomaterials Science – An Introduction to Materials in Medicine, vols. 2.3 and 7.19, Elsevier, London, UK, 2004, pp. 697–707, 80–86.
[7] K. Gao, L. Li, L. He, K. Hinkle, Y. Wu, J. Ma, L. Chang, X. Zhao, D.G. Perez, S. Eckardt, J. McLaughlin, B. Liu, D.F. Farson, L.J. Lee, Design of a microchannel-nanochannel-microchannel array based nanoelectroporation system for precise gene transfection, Small 10 (5) (2014) 1015–1023.
[8] H. Huang, Z. Guo, Ultrashort pulsed laser ablation and stripping of freeze-dried dermis, Lasers Med. Sci. 25 (4) (2010) 517.
[9] C. Hassler, T. Boretius, T. Stieglitz1, Polymers for neural implants, J. Polym. Sci. Part B: Polym. Phys. 49 (1) (2011) 18–33.
[10] G. Liang, G.S. Guvanasen, L. Xi, C. Tuthill, T.R. Nichols, S.P. DeWeerth, A PDMS-based integrated stretchable microelectrode array (is MEA) for neural and muscular surface interfacing, IEEE Trans. Biomed. Circuitsand Syst. 7 (1) (2013) 1–10.
[11] M. HajjHassan, V. Chodavarapu, S. Musallam, Review: NeuroMEMS: neural probe microtechnologies, Sensors 8 (10) (2008) 6704–6726.
[12] S. Lacour, S. Benmerah, E. Tarte, J. Fitz Gerald, J. Serra, S. McMahon, J. Fawcett, O. Graudejus, Z. Yu, B. Morrison, Flexible and stretchable micro-electrodes for in vitro and in vivo neural interfaces, Med. Biol. Eng. Comput. 48 (10) (2010) 945–954.
[13] M. Schuettler, S. Stiess, B.V. King, G.J. Suaning, Fabrication of implantable microelectrode arrays by laser cutting of silicone rubber and platinum foil, J. Neural Eng. 2 (1) (2005) S121.
[14] G. Liang, G.S. Guvanasen, L. Xi, C. Tuthill, T. Richard Nichols, S.P. DeWeerth, A PDMS-based integrated stretchable microelectrode array (isMEA) for neural and muscular surface interfacing, IEEE Trans. Biomed. Circuits Syst. 7 (1) (2013).
[15] S. Maruo, O. Nakamura, S. Kawata, Three-dimensional microfabrication with two-photon-absorbed photopolymerization, Opt. Lett. 22 (1997) 132–134.
[16] L.D. Laude, C. Cochrane, Cl. Dicara, C. Dupas-Bruzek, K. Kolev, Excimer laser decomposition of silicone, Nucl. Instrum. Meth. Phys. Res. B 208 (2003) 314–319.
[17] Cl. Dicara, T. Robert, K. Kolev, C. Dupas-Bruzek, L.D. Laude, Excimer laser processing of silicone rubber: from understanding the process to applications, Proc. SPIE 5147 (2003) 255–265.
[18] V.-M. Graubner, O. Nuyken, Th. Lippert, A. Wokaun, S. Lazare, L. Servant, Local chemical transformations in poly(dimethylsiloxane) by irradiation with 248 and 266 nm, Appl. Surf. Sci. 252 (13) (2006) 4781–4785.
[19] K. Rubahn, J. Ihlemann, G. Jakopic, A.C. Simonsen, H.-G. Rubahn, UV laser-induced grating formation in PDMS thin films, Appl. Phys. A 79 (2004) 1715–1719.
[20] C. Dupas-Bruzek, O. Robbe, A. Addad, S. Turrell, D. Derozier, Transformation of medical grade silicone rubber under Nd:YAG and excimer laser irradiation: first step towards a new miniaturized nerve electrode fabrication process, Appl. Surf. Sci. 255 (21) (2009) 8715–8721.
[21] S. van Pelt, A. Frijns, R. Mandamparambil, J. den Toonder, Local wettability tuning with laser ablation redeposits on PDMS, Appl. Surf. Sci. 303 (2014) 456–464.
[22] H. Huang, L.-M. Yang, J. Liu, Nanofabrication with UV femtosecond fiber laser, Abstract Number: 227, in: Natotech Conference & Expo 2012, 18–21 June, Santa Clara, CA, USA, 2012.
[23] P.A. Atanasov, N.N. Nedyalkov, E.I. Valova, Z.S. Georgieva, S.A. Armyanov, K.N. Kolev, S. Amoruso, X. Wang, R. Bruzzesse, M. Sawczak, G. Sliwinski, Fs-laser processing of polydimethylsiloxane, J. Appl. Phys. 116 (2) (2014) 023104.
[24] S. Darvishi, T. Cubaud, J.P. Longtin, Ultrafast laser machining of tapered microchannels in glass and PDMS, Opt. Lasers Eng. 50 (2012) 210–214.
[25] C.L. Sones, I.N. Katis, B. Mills, M. Feinaeugle, A. Mosayyebi, J. Butement, R.W. Eason, Rapid and mask-less laser-processing technique for the fabrication of microstructures in polydimethylsiloxane, Appl. Surf. Sci. 298 (2014) 125–129.
[26] A. Zukauskas, G. Bataviciute, M. Sciuka, T. Jukna, A. Melninkaitis, M. Malinauskas, Characterization of photopolymers used in laser 3D micro/nanolithography by means of laser-induced damage threshold (LIDT), Opt. Mater. Express 4 (8) (2014) 1601–1616.
[27] L.D. Laude, EP 1995/0693138 A1; US 1997/5599592 A; US 2008/0305320 A1.
[28] N.E. Stankova, P.A. Atanasov, N.N. Nedyalkov, T.R. Stoyanchov, K.N. Kolev, E.I. Valova, J.S. Georgieva, St.A. Armyanov, S. Amoruso, X. Wang, R. Bruzzese, K. Grochowska, G. Œliwiñski, K. Baert, A. Hubin, M.P. Delplancke, Fs- and Ns-laser processing of polydimethylsiloxane (PDMS) elastomer: comparative study, Appl. Surf. Sci. 336 (2015) 321–328.
[29] R. Srinivasan, B. Braren, K.G. Casey, Nature of “incubation pulses” in the uitraviolet laser ablation of polymethyl methacrylate, J. Appl. Phys. 68 (4) (1990) 1842–1847.
[30] S.R. Cain, F.C. Burns, C.E. Otis, On single-photon ultraviolet ablation of polymeric materials, J. Appl. Phys. 71 (9) (1992) 4107–4116.

[31] V. Srinivasan, M.A. Smrtic, S.V. Badu, Excimer laser etching of polymers, J. Appl. Phys. 59 (11) (1986) 3861–3867.
[32] G.B. Blanchet, P. Cotts, C.R. Fincher, Incubation: subthreshold ablation of poly-(methyl methacrylate) and the nature of the decomposition pathways, J. Appl. Phys. 88 (5) (2000) 2975–2978.
[33] Th. Lippert, Laser application of polymers, Adv. Polym. Sci. 168 (2004) 51–246.
[34] S.C. Bae, H. Lee, Z. Lin, S. Granik, Chemical imaging in a surface forces apparatus: confocal Raman spectroscopy of confined poly(dimethylsiloxane), Langmuir 21 (13) (2005) 5685–5688.
[35] C. Palma, M.C. Rossi, C. Sapia, E. Bemporad, Laser-induced crystallization of amorphous silicon–carbon alloys studied by Raman microscopy, Appl. Surf. Sci. 138–139 (1999) 24–28.
[36] Y. Ward, R.J. Young, R.A. Shatwell, A microstructural study of silicon carbide fibres through the use of Raman microscopy, J. Mater. Sci. 39 (2004) 6781.
[37] A.C. Ferrari, Raman spectroscopy of graphene and graphite: disorder, electron–phonon coupling, doping and nonadiabatic effects, Solid State Commun. 143 (2007) 47–57.
[38] S. Ona, Y. Nakamoto, T. Kagayama, K. Shimizu, Y. Nishikawa, M. Murakami, K. Kusakabe, T. Watanuki, Y. Ohishi, Stability of hexagonal diamond under pressure, J. Phys. Conf. Ser. 121 (2008) 062006.
[39] V.Y. Yadav, D.K. Sahu, K. Devendra, M. Singh, K. Kumar, Study of Raman spectra of nano-crystalline diamond like carbon (DLC) films composition (sp2:sp3) with substrate temperature, in: Proceedings of the World Congress on Engineering and Computer Science, 2009, vol. I, WCECS 2009, October 20–22, San Francisco, USA, 2009.